CrossMark

Two centuries temperature variations over subtropical southeast China inferred from *Pinus taiwanensis* Hayata tree-ring width

QiuFang Cai[1] · Yu Liu[1,2,3]

Abstract High-resolution long-term temperature reconstructions in subtropical southeast China (SSC) are very scarce, yet indispensable for the comprehensive understanding of climate change in China, even in East Asia. We reconstructed the first previous growth-season temperature in the Sanqingshan Mountains (SQS), southeast China since 1806 based on tree-ring width data. The reconstruction accounts for 56.4 % of the total variance in the instrumental record over 1954–2009. Unlike the Northern Hemispheric warming during recent two centuries, the reconstruction captured a slowly cooling trend from 1806 to 1980, followed by a rapid warming afterward. 2003–2009 was the warmest period in the reconstruction. 1970–2000 was colder than the last stage of the Little Ice Age (LIA). Most of the warm and cold periods in this reconstruction could be found in the tree-ring based temperature reconstructions of vicinity area, indicating that the temperature variations in SSC were almost synchronous at least at decadal scale. This regional coherence of temperature variation was further confirmed by the spatial correlation patterns with the CRU TS3.22 grid dataset. A strong positive relationship between the temperature over SQS region and sea surface temperature (SST) over the North Pacific Ocean (NP) has been noted, suggesting that SST variations over NP and the related Pacific Decadal Oscillation significantly influenced the temperature variability over SSC. To better understand the climate variability during the LIA and the regional differences in temperature variations over SQS and northern Hemisphere, long data sets from more diverse areas of southern China are needed.

✉ QiuFang Cai
caiqf@ieecas.cn

✉ Yu Liu
liuyu@loess.llqg.ac.cn

1   The State Key Laboratory of Loess and Quaternary Geology, Institute of Earth Environment, Chinese Academy of Sciences, Xi'an 710075, China

2   Joint Center for Global Change Studies (JCGCS), Beijing Normal University, Beijing 100875, China

3   Department of Environment Science and Technology, School of Human Settlements and Civil Engineering of Xi'an Jiaotong University, Xi'an 710049, China

1 Introduction

Temperature is one of the most important factors of global climate change. How temperature will change in the future is greatly concerned by governments and publics. Due in part to inadequate long-term observation, our knowledge of past temperature change mainly comes from natural proxies (ice-cores, Speleothem, historical documents, tree rings, etc.) (Christiansen and Ljungqvist 2012; PAGES 2k Consortium 2013; Shi et al. 2013), which is fundamental for future climate projections.

Well replicated, accurately dated and annually resolved tree rings serve as one of the most important palaeoclimatic archives, and have provided unique insight into the nature of past climate variability in the pre-instrumental era. As time goes on, more and more long-term regional-, even hemispheric-scale climate have been reconstructed based on improved local (site) tree-ring materials (Esper et al. 2002; Büntgen et al. 2011; Seftigen et al. 2013; Cook et al. 2013; Yang et al. 2014; Zhang et al. 2015). In spite of the similar climate pattern in different sites (or regions),

there are still large disparities among the many existing reconstructions, leading to an uncertainty in the timing and amplitude of past climate change (Linderholm et al. 2015). Moreover, the insufficient spatiotemporal distribution of the tree rings used by these large-scale reconstructions may also limit empirical assessments of regional or hemispheric variability and make the reconstructions imperfect (Li et al. 2015b). Therefore, more independent tree-ring studies from different climatic zone are necessary to gain a thorough understanding of the regional and hemispheric climate variability.

Subtropical southeast China (hereafter SSC, 22–34°N, >98°E) is a high-speed economic development region in China and is densely populated (population accounts for about half of the total population). It belongs to the warm and humid subtropical maritime monsoon climate. The annual mean temperature generally ranges from 17 to 21 °C, and the annual mean precipitation is about 1400–2000 mm. In recent years, climate anomalies and natural disasters frequently occurred in this region and severely threatened people's life and property safety, as well as the social economic development (Ding et al. 2008). There is an urgent need to investigate the long-term climate history to understand the characteristics and causes of climate variation. Before 2010, tree-ring width based climate reconstructions in SSC were scarce due to dating difficulty, as well as the complicated relationship between tree rings and climatic factors on one hand. On the other hand, SSC is not taken seriously because of the general understanding that subtropical regions are less sensitive to climate change and potentially have less impact on local climate than the arid to semi-arid regions (Duan et al. 2015; Rotenberg and Yakir 2010). However, studying of the climate variation in SSC is indispensable for the comprehensive understanding of the climate change in East Asia. During recent years, there has been increasing evidences of the climatic potential of tree rings in this region (Zheng et al. 2012; Chen et al. 2015). Most studies focused on the winter-time temperature reconstructions (Shi et al. 2010; Chen et al. 2012; Duan et al. 2012), few on growth seasons. However, growth season temperatures are more crucial than the winter-time temperatures for the vegetation growth and agricultural production (Shi et al. 2015b). For instance, temperature variation during growth season can change the suitable rice cropping areas, cropping systems and crop water requirements in southern China (Ye et al. 2015). High temperature above the tolerance threshold of crop growth can cause heat stress and therefore result in dramatic yield reductions (Liu et al. 2013).

Pinus taiwanensis Hayata is an important afforestation tree species in the middle and lower reaches of the Yangtze River region, southeast China, and has been demonstrated to be valuable in reconstructing historical climate (Chen et al. 2012; Duan et al. 2012). It is a photophilous, deep rooted plant, mainly grows on the limestone mountainous area at the elevation from 600 to 1800 m a.s.l., and generally grows well in conditions with relatively high humidity. A previous study in southeast China indicated that the growth season of this species may happen during April–November (He et al. 2012). In the present paper, *Pinus taiwanensis* tree-ring cores from the high elevation site of the Sanqingshan Mountains (SQS) were collected. We aim to: (1) examine the potential of *Pinus taiwanensis* Hayata as a proxy of past temperature variability, (2) develop a new growth-season temperature reconstruction in southeast China over the last two centuries, and (3) tentatively discuss the possible causes of temperature variability in southeast China. We anticipate that our reconstruction will not only help to increase the network of temperature sensitive tree-ring chronologies in this region, but also help to predict the possible impact of future climate change on *Pinus taiwanensis* for forest management purpose.

2 Materials and methods

2.1 Study area and climatic data

SQS (Fig. 1) is located in the middle reaches of Yangtze River, northeast Jiangxi Province of the subtropical southeast China. The main body of the mountains is about 12.2 km stretching from north to south, and 6.3 km from west to east. It has a flat shape of a lotus leaf, and tilts from southeast to northwest. The bedrock of this mountain is mainly composed of granite, formed in the late Yanshanian period (Yin et al. 2007). After that, it experienced long-term erosion and denudation, forming a landscape of deep-incised valleys, steep cliffs and stone columns and peaks standing upright as trees. The highest peak of SQS is Yujng peak, about 1816 m a.s.l.

SQS is characterized by subtropical monsoon climate, with mountainous climate characteristic, and is characterized by four distinct seasons. Instrumental temperature from Yushan (28°41′ N, 118°15′ E, 116.3 m a.s.l., 1951–2009), the nearest meteorological station (about 30 km southeast of SQS), ranges from 5.52 °C in January to 29.03 °C in July. The annual precipitation is 1819.31 mm, annual mean evaporation is about 1332 mm, and the humidity is relatively high (82 %) (Yin et al. 2007). We estimate that the temperatures at the SQS sampling site (1545 m a.s.l.) is about 8.5 °C colder than Yushan station (about 1400 m lower) based on the altitude effect, and precipitation increases greatly at the sampling site accordingly. Obviously, the sampling site is characterized by cool-humid condition. Temperature should be the limiting factor of tree growth.
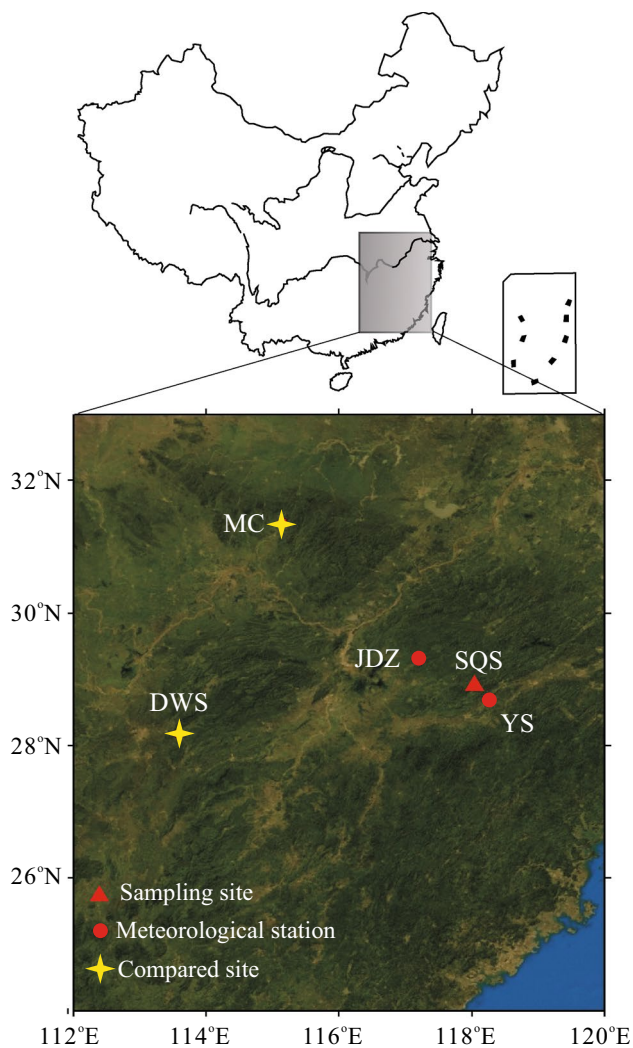
Fig. 1 Map showing the general locations of the sampling site (*triangle*), meteorological stations (*dots*) and compared sites (*stars*). *SQS* Sanqingshan Mountains, *JDZ* Jingdezhen, *YS* Yushan, *DWS* Daowushan Mountain (Shi et al. 2015a); *MC* Macheng (Cai and Liu 2013)

Monthly climatic data including precipitation, maximum, mean and minimum temperatures are extracted from Yushan station and Jingdezhen (29°18′ N, 117°12′ E, 61.5 m, 1953–2009) station, respectively. The Jingdezhen station is about 100 km northwest of the study area. Figure 2 shows that the climatic factors of the two stations, temperature in particular, are accordant to each other, showing great similarity of climate in a larger area around the sampling site. Therefore, the climate data from these two meteorological stations were arithmetically averaged to represent the regional climate (1953–2009). The hottest months were found in July and August. 81 % precipitation concentrated on March through October. Although great difference exists between the altitudes of the meteorological stations and the sampling site, the climatic records in the stations are thought confident indicators of the conditions at the higher elevation and hence can be used for the calibration in the dendroclimatic reconstructions based on high-elevation tree-ring data (Liang et al. 2011).

2.2 Tree-ring data

The sampling site is located near the upper forest border of *Pinus taiwanensis* in SQS (28.9° N, 118.05° E, 1545 m). In the sampling site, *Pinus taiwanensis* is the dominant tree species and accompanied by dense shrubs and bamboos. The environment of the sampling site is comparatively open. The trees grow in thick layer of mountain yellow brown soil, which is rich in organic matter. In June 2010, we collected 62 tree-ring cores from 35 healthy *Pinus taiwanensis* using increment borer at breast height, with one or two cores from each tree. When we collected tree-ring cores, we tried to get to the pith to maximize our sample ages.

All the samples were dealt with standard dendrochronological method (Cook and Kairiukstis 1990), including air-drying, mounting, polishing with progressively finer sand paper to make the ring boundary discernable. Then visual crossdating was adopted to preliminarily assign the calendar years to each growth ring. The width of each annual ring from all the cores was measured using LINTAB machine to the nearest 0.01 mm, and the results of measurement and crossdating were further checked by the program COFECHA (Holmes 1983). The successfully cross-dated series were then conservatively standardized to remove non-climate trends due to tree age and stand dynamics via the ARSTAN program (Cook 1985). To retain as much low frequency as possible, negative exponential curve or straight line of negative slope, or horizontal line was applied to each tree-ring series. The raw data of each ring was divided by the corresponding year's value of the fitted curve to give a dimensionless index. Finally, the standard chronology was generated by averaging all the indices (Fig. 3). In order to minimize the effect of sample size, the variance of the chronology was stabilized during the chronology development based on the Briffa Rbar-weighted method (Osborn et al. 1997). We adopted the threshold of 0.85 by Sub-sample signal strength (SSS) (Wigley et al. 1984) to determine the reliable starting year of chronology, neglecting the low quality earlier years due to low sample size. Common interval analysis of the chronology was conducted between 1830–2000 AD (Table 1). The evaluated parameters included the mean sensitivity (MS), standard deviation (SD), first-order autocorrelation (AR1), correlation coefficients among all series (r_1), between trees (r_2) and within trees (r_3), the expressed population signal (EPS), variance in first eigenvector (PC1) and signal-to-noise ratio (SNR).
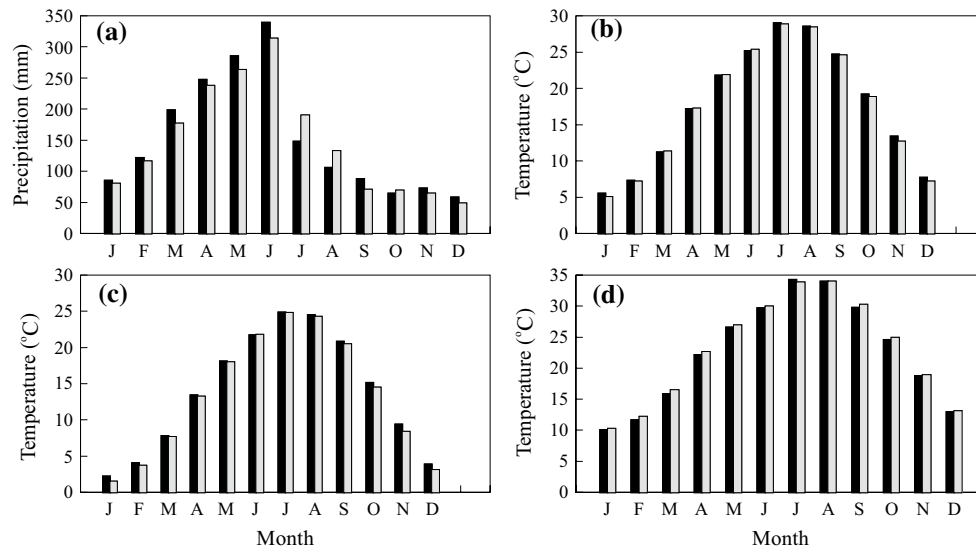
Fig. 2 Monthly distribution of precipitation amount (**a**), mean temperature (**b**), mean minimum temperature (**c**) and mean maximum temperature (**d**) records of Yushan station (*black bar*) and Jingdezhen station (*light bar*)
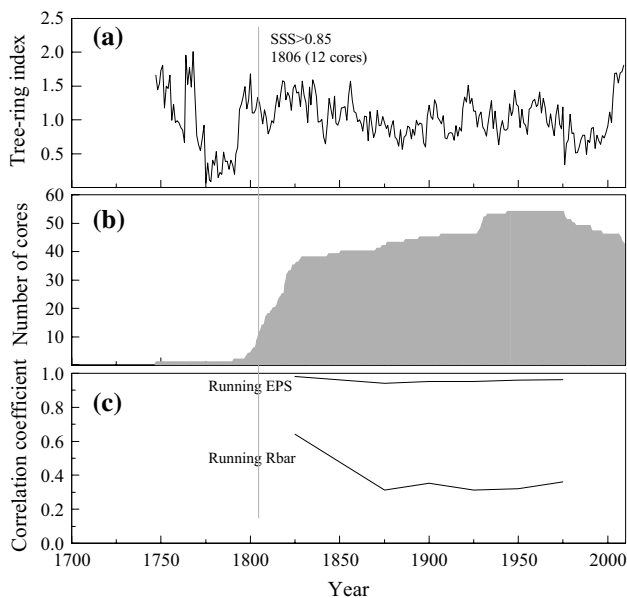

Fig. 3 a The tree-ring chronology of the Sanqingshan Mountains, **b** number of cores and **c** running EPS and Rbar statistics

2.3 Climate-growth analysis and temperature reconstruction

Tree growth-climate relationship was detected by the Pearson correlation analysis between tree-ring index of *Pinus taiwanensis* and climatic factors from the two stations, as well as the regional climate. The high AR1 of tree-ring chronology indicated that previous year climate also had significant effect on tree growth of the following year, thus

climatic data including 22 months from previous January to current October were used in the following tree growth-climate analysis. Based on this analysis, the limiting climatic factor was reconstructed. The fidelity of reconstruction was checked by the split calibration-verification cross check (Meko and Graybill 1995). The statistical parameters for assessment include the Pearson's correlation coefficient (*r*), R-squared (R^2), sign test (ST), reduction of error (RE) and coefficient of efficiency (CE) (Fritts 1976; Cook et al. 1999). Here RE and CE have a theoretical range of $-\infty$ to $+1$, respectively. Usually positive RE and CE indicate reconstruction skill in excess of the verification period climatology, and negative RE and CE indicate less skill than verification period climatology (Cook et al. 1999).

The spatial pattern of the reconstructed temperature was investigated through the spatial correlation analysis with CRU TS3.22 gridded concurrent temperatures (http//www.knmi.nl) over the period of 1954–2009. Comparison of the reconstructed temperature with nearby tree-ring based temperature reconstructions was further conducted to support the spatial representativeness of the reconstruction.

3 Results

3.1 Tree-ring chronology

After series with short age or ambiguity are discarded, 54 cores from 34 trees are successfully cross-dated with the mean series intercorrelation of 0.55. There are 35 tree-ring cores were dated back at least to 1828. 8 series are less than 100 years because the early parts were twisted too much

Table 1 Statistics of the tree-ring index and common period (1830–2000 AD) analysis

Mean sensitivity (MS)	0.218
Standard deviation (SD)	0.319
First-order autocorrelation (AR1)	0.677
SSS > 0.85	1806–2009
Mean correlation among all series (r_1)	0.235
Mean correlation between trees (r_2)	0.230
Mean correlation within trees (r_3)	0.421
Expressed population signal (EPS)	0.915
Variance in first eigenvector (PC1)	28.99 %
Signal-to-noise ratio (SNR)	10.812

and undiscernable. As shown in Fig. 3, the resulting tree-ring chronology spans from 1747 to 2009, whereas the reliable chronology only covers the time interval of 1806–2009, with a mean length of series of 167.4 years. The high value of each parameter in Table 1 denotes the reliable quality of the chronology for further analysis. Among them, the high values of correlation coefficients (r_1, r_2, r_3), SNR, PC1 and EPS indicate the strength of the common signal contained in all the ring-width series from each

individual core. MS is a metric to evaluate the variance between adjacent ring widths, high value of MS suggests that tree rings are sensitive to external force (e.g. climate), and more climatic information is possibly retained in the chronology. The MS value in this study is 0.218, which could meet the general requirement of dendroclimatology in southeast China (Zheng et al. 2012; Shi et al. 2015a). The running Rbar (moving correlations among series) is above 0.31 during the whole period of chronology, and the running expressed population signal (EPS) values are above 0.9, indicating good quality of this chronology (Wigley et al. 1984).

3.2 Climate-growth relationship

The tree-ring width chronology has statistically similar response to the climatic factors in both stations (Fig. 4). The obvious feature is that tree rings respond to monthly (maximum and mean, in particular) temperatures much stronger than to monthly precipitation. The tree-ring chronology has positive correlations with both current and previous years' monthly maximum mean temperatures in March, April, June, July and September at the 0.01 significant levels. On the seasonal scale, the tree-ring chronology
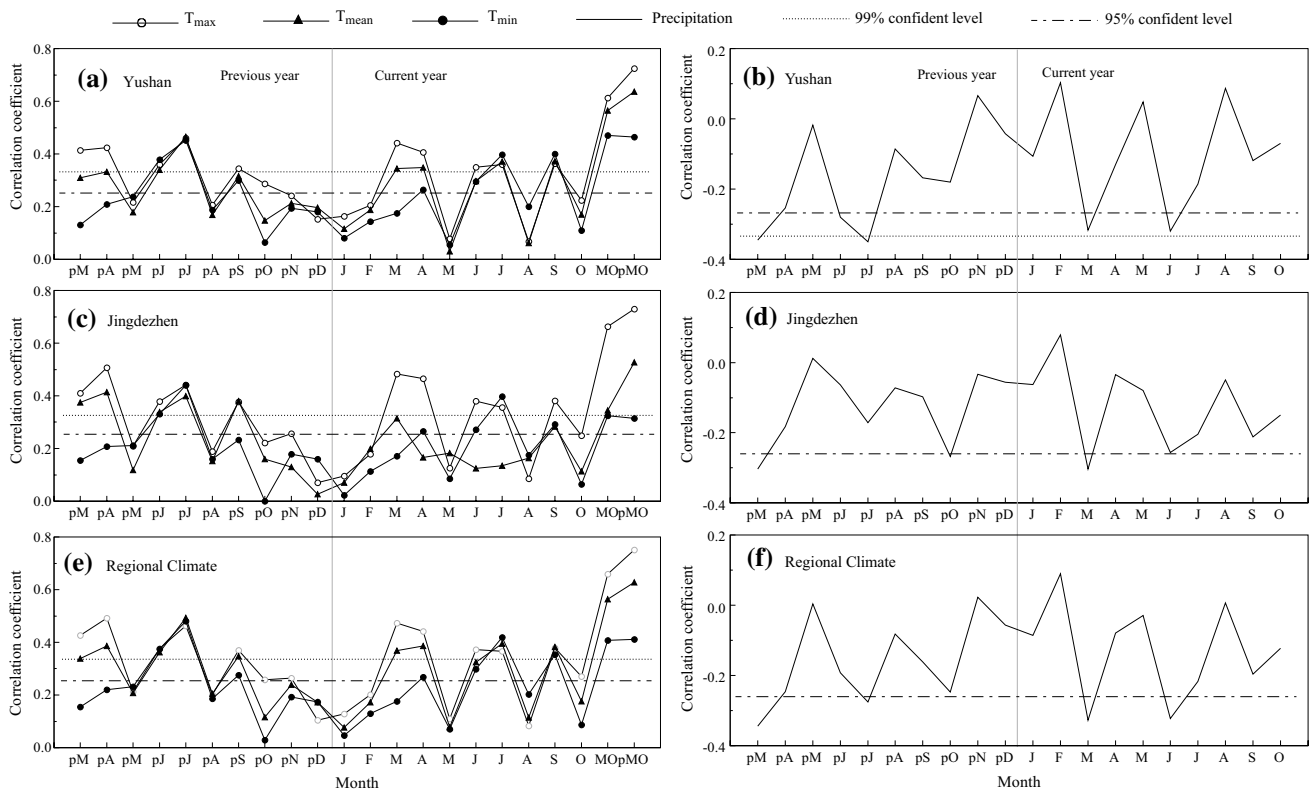

Fig. 4 Correlation coefficients between the tree-ring chronology of SQS and climatic factors at Yushan (**a**, **b**), Jingdezhen (**c**, **d**) meteorological stations and the regional climate (**e**, **f**). P denotes previous year; MO denotes the season from March to October of current year (t); pMO denotes the season from previous (t − 1) March to previous October
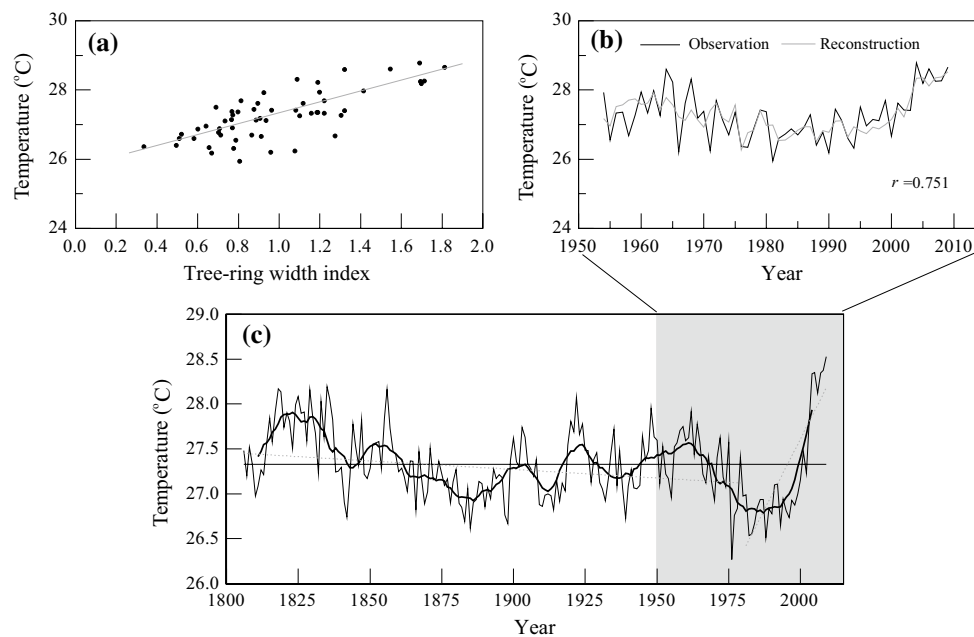
Fig. 5 a Scatter plot of the tree-ring width index and the maximum mean temperature of pMO; **b** Comparison between the reconstructed and observed maximum mean temperature of pMO during the common period of 1954–2009; **c** Reconstruction of the maximum mean temperature of pMO from 1806 to 2009 (*thin curve*). The *bold black curve* indicates the 11-year moving average of the reconstruction; the *straight thin line* indicates the average value of the reconstruction from 1806 to 2009; the *dashed lines* indicate the cooling and warming trend, respectively

indicated very high correlations with the regional maximum mean temperatures from March to October of current growth year ($r = 0.66$, $p < 0.001$) and from previous March to previous October ($r = 0.751$, $p < 0.001$). Moreover, the tree-ring chronology also showed significant correlations with regional annual mean maximum temperature from previous July to current June with $r = 0.72$ ($p < 0.001$).

In contrast, the tree-ring chronology shows weak correlations with monthly and seasonal precipitation amounts. It only has significant correlations ($p < 0.01$) with monthly precipitations in previous March, July at Yushan station, and has significant correlations ($p < 0.05$) with monthly precipitation in previous June, current March and June in Yushan station, previous March, October and current March in Jingdezhen station, respectively.

3.3 Maximum temperature reconstruction of previous March–previous October

The multiple linear regression Eq. (1) considering both the maximum mean temperature of current March–October (T_{max-MO}) and previous March–previous October ($T_{max-pMO}$) can explain 72.3 % of the variance of tree-ring width (STD_t).

$$STD_t = 0.208 \times T_{max-MO} + 0.284 \times T_{max-pMO} - 12.431 \tag{1}$$

$r = 0.851$, $r^2 = 72.3$ %, $r^2_{adj} = 71.3$ %, $F = 69.314$, $p < 0.001$.

If we control the $T_{max-pMO}$, the correlation coefficient between tree-ring chronology and T_{max-MO} is 0.605 ($p < 0.001$), and the correlation coefficient is 0.701 ($p < 0.001$) between tree-ring chronology and $T_{max-pMO}$ when T_{max-MO} is controlled. It robustly confirmed that both the maximum temperatures of previous March–previous October and current March–October significantly influenced tree growth in SQS region, and the influence of climate in the previous year was superior to current year.

Therefore, a simple linear regression model (2) is designed to reconstruct the previous growth season maximum mean temperature ($T_{max-pMO}$) as

$$T_{max-pMO} = 1.529 \times STD_t + 25.757 \tag{2}$$

$N = 56$, $r = 0.751$, $r^2 = 56.4$ %, $r^2_{adj} = 55.6$ %, $F = 69.821$, $p < 0.001$.

The reconstruction can explain 56.4 % of the variance in the instrumental records. Figure 5a indicates that there exists good linear relationship between the tree-ring width index and $T_{max-pMO}$. The reconstruction simulates the observed temperature over their common period 1954–2009 in good skill (Fig. 5b).

As shown in Table 2, the r values at both the calibration and verification periods are significant ($p < 0.01$), and r values of later periods are stronger than the earlier periods. The strengthening relationship between tree rings and the target factor during recent modeling period was also

Table 2 Calibration and verification statistics for the tree-ring reconstruction of the previous March–October maximum mean temperature

	Calibration (1954–1983)	Verification (1984–2009)	Calibration (1980–2009)	Verification (1954–1979)	Full calibration (1954–2009)
r	0.584**	0.884**	0.857**	0.558**	0.751**
R^2	0.341	0.781	0.735	0.312	0.564
RE	–	0.761	–	0.292	–
CE	–	0.752	–	0.291	–
Sign test		22 +/4-**		19 +/7-*	–

*, ** Significance at the 95 and 99 % confidence levels, respectively

widely reported in elsewhere of China (Fang et al. 2010; Chen et al. 2013; Cai et al. 2015). Similar to the r values, the results of sign test at each verification period were significant, and the significance of the latter period is higher than the earlier period. Moreover, RE and CE, the two rigorous verification statistics showed positive values, indicating enough skill in the regression model.

Based on the above regression model (2), the maximum mean temperature of previous March–October in SQS region was reconstructed back to 1806 (Fig. 5c), greatly extended the instrumental record. The reconstruction indicated considerable variability on annual to multi-year episodes of cool and warm, with the mean value of 27.33 °C and standard deviation (σ) of 0.42 °C.

4 Discussions

4.1 The limiting factor for tree growth

Previous study in the adjacent Zhejiang province, southeast China suggested that the growth season of coniferous tress generally started in early April and ended in early November (He et al. 2012), and the start day usually delayed with elevation increase, while the end day remained stable. Therefore, March–October roughly covers the whole growth season of *Pinus taiwanensis* in SQS and the tree growth-climate relationship is meaningful in terms of tree physiology.

For most tree species, the lowest temperature for phytosynthesis is 5–8 °C, the most suitable temperature is 25–30 °C (Pan 2007). Generally the tree growth will enhance with the increase of temperature in a certain temperature range. The location of our sampling site is on the top of the SQS Mountains, where the monthly mean temperature ranges from −2.98 to 20.53 °C, deduced from the temperature record of Yushan station (about 1400 m lower) based on the adiabatic lapse rates. In the sampling site, March is the first month of a year with average temperature above 5 °C, and the highest temperature during a year is in July (20.53 °C). Therefore, warm temperatures in spring

can stimulate the meristematic activities in the following growth season to start early and result in a prolonged growth season, and warm temperature during growth season is in favor of the photosynthetic activity of trees and therefore accelerates tree growth. In one word, trees can benefit from the warm climate during March–October and produce wide rings in growth seasons in study site of SQS region, and vice versa. Our result meets the general assumption that trees growing at high elevation or high latitude were temperature limited (Yadav et al. 1999; Liang et al. 2008; Davi et al. 2015).

The annual precipitation in study site is above 1820 mm. Compared with the strong limitation of temperature, precipitation has weak impact on tree growth. *Pinus taiwanensis* is a photophilous species. Too much precipitation during growth or pre-growth season can greatly reduce the sunshine radiation that is favorable for leaf photosynthesis on one hand. On the other hand, it can also lower the maximum temperature during the daytime. Moreover, cloud generally comes along with precipitation. The clouds cover can obscure the sun and block the direct rays of the sun (Suehrcke 2000). When the cloud cover is thick, it can significantly reduce the level of radiation received on the earth's surface and result in low temperature, and vice versa. A further spatial correlation pattern indicated that the maximum temperature in SQS region was negatively related to the cloud cover over the study area (Fig. 6d).

Tree growth is subjected not only to the influence of current year climate, but also previous years (Fritts 1976). The earlywood formed and manufactured during the early period of growth season at least partly uses stored photosynthate from previous year (McCarroll and Loader 2004). In the present work, both current and previous years' temperatures limited tree growth, and the prior March–October temperature imposed much stronger influence on tree growth than that of current year. The lag effect of temperature on tree growth has been widely reported for different species (Davi et al. 2015). In northwest China, the whole previous year temperature was the limiting factor for Qilian juniper (Liu et al. 2009). In southeast China, wintertime temperature limitation before the growth season was
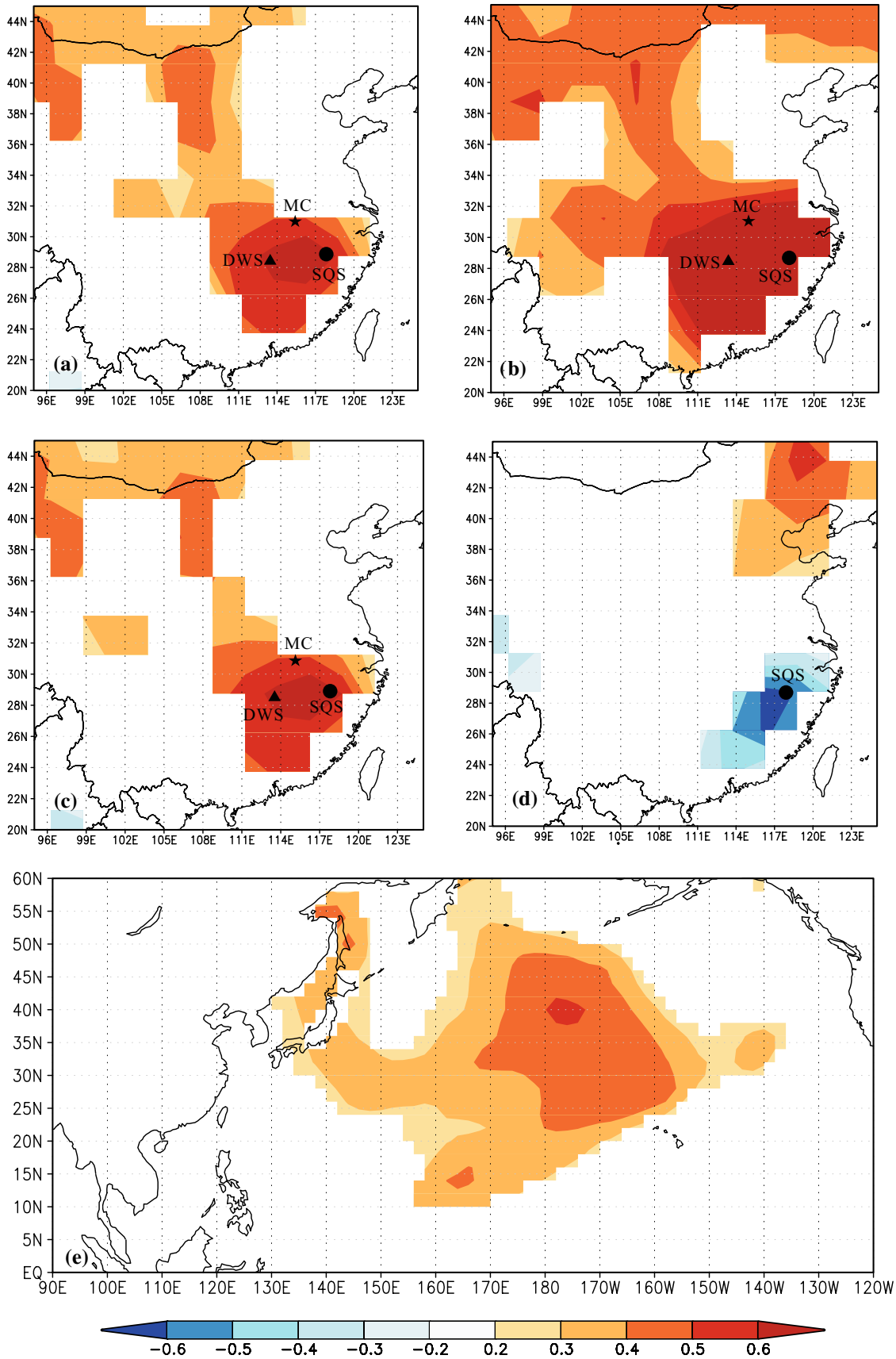
Fig. 6 Spatial correlation patterns of the reconstructed **a** and observed **b** $T_{max-pMO}$ with the concurrent CRU TS3.22 land maximum temperature grid dataset (http://climexp.knmi.nl), **c** Spatial correlation patterns of the detrended $T_{max-pMO}$ reconstruction and the CRU TS3.22 land grid dataset, the spatial correlation pattern of **d** the reconstruction with the cloud cover and **e** global sea surface temperatures (SST) over their common period (1954–2009). MC represents Macheng (Cai and Liu 2013), DWS represents Daowushan (Shi et al. 2015a)

mostly reported (Shi et al. 2010; Duan et al. 2012; Chen et al. 2012). The previous study in two different regions of southeast China also reported that tree-ring width growth of *Pinus taiwanensis* was strongly related to the mean temperature of June and July of previous year in positive phase (Li et al. 2014), and the lag effect of prior temperature on tree growth was stronger than current year climatic factors.

4.2 Temperature variability through time

The reconstruction exhibits obvious decadal-scale variation after 11-year moving average smoothing. There are four evident cold periods in the reconstruction including 1860–1898, 1909–1918, 1930–1944 and 1970–2000, and five warm periods including 1814–1837, 1844–1858, 1919–1926, 1945–1965 and 2003–2009. Among them, 2003–2009 is the warmest period in the reconstruction, about 0.93 °C higher than the mean temperature for the whole reconstruction (1806–2009), and 0.97 °C higher than the mean temperature for the instrumental period (1954–2009). 1970–2000 (mean value was 26.93 °C) is the coldest period in the reconstruction, about 0.40 °C lower than the mean temperature for the whole reconstruction, and 0.36 °C lower than the mean for the instrumental period.

Another obvious feature of the reconstruction is that the temperature in SQS experienced a slowly cooling process from 1806 to 1980 (the slope is −0.0019), which was interrupted by a slow warming during 1885–1948. The cooling trend in SQS is opposite to the warming trends in elsewhere of Asia (Pages 2K Consortium 2013; Davi et al. 2015) and Northern Hemisphere (Mann et al. 2009). Moreover, our reconstruction indicates significantly negative correlation with the observed Northern hemisphere maximum mean temperature of previous March–October (http://www.cru.uea.ac.uk/cru/data/tem2/tavenh2v.dat) during 1856–1997 ($r = -0.274$, $p < 0.001$). Even during the instrumental period, the SQS region didn't exhibit direct warming. It underwent a cooling trend from 1962 to 1980, followed by an abrupt warming since 1981. The cooling trend of climate reported here was not the first case. Similar to our result, Yadav and Singh (2002) has reported a long-term cooling trend of spring temperature in western Himalaya, which started from the late 17th century and ended early in the 20th century. Even during the latter part of

the 20th century, western Himalayas defied global warming (Yadav et al. 2004). Moreover, the recent two centuries warming trend wasn't captured by the tree rings on the eastern Tibetan Plateau (Xing et al. 2014). Global climate change is complex. Regional climate changes are largely independent, rather than globally synchronous change. The existence of such regional differences in temperature variations over different geographic regions warrants the need to develop long data sets from more diverse areas of the world to achieve a more accurate hemispheric view of climate change (Yadav and Singh 2002).

The early-half of the 19th century belongs to the last stage of Little Ice Age (LIA), but in the SQS region, the reconstructed temperature wasn't low. In contrary, it exhibited warm stage, showing difference from the global climate (Pages 2K Consortium 2013; Davi et al. 2015). 1860–1898 was the second coldest period in our reconstruction. It is consistent with the timing of the coldest stage of the LIA (1861–1890) in China (Ge 2011). Coincidentally, 1860–1900 is also the high-incidence years of frozen injury of citrus in the middle and lower reaches of the Yangtze River (Gong and Zhang 1983; Ge 2011), evidencing the low temperature during this period over southeast China. The LIA has been conventionally defined as a period extending from the sixteenth to the nineteenth centuries (Michael 2003) or alternatively, from about 1300 to about 1850 (Matthews and Briffa 2005). However, several controversial issues remain including the timing of the onset (and end) of the LIA and the amplitude and timing of temperature variations within the LIA (Matthews and Briffa 2005). In China, Zheng et al. (2002) defined the timing of the LIA from 1501 to 1910, and the temperature variability during LIA was regional independent (Wang et al. 1998). Therefore, the high temperature during the early 19th century in this study could be a warm fluctuation during the LIA, and 1860–1898 only represented a cold period, instead of the coldest period during LIA in the study area. This finding supports that LIA was a period of fluctuating climatic conditions, rather than a long period of several centuries of sustained cold (Bradley and Jones 1993). The above analysis indicates that our temperature reconstruction in SQS remains considerable hemispheric temperature signal, while also shows great difference to the large-regional temperature variation.

4.3 Spatial representativeness and comparison with other records

The reconstruction has a considerable spatial representativeness as shown in Fig. 6a, which simulates the spatial field correlation between the instrumental temperature and concurrent global temperature (Fig. 6b) to a certain degree. In order to eliminate the illusion caused by trend correlation, the linear trends of the reconstruction and grid
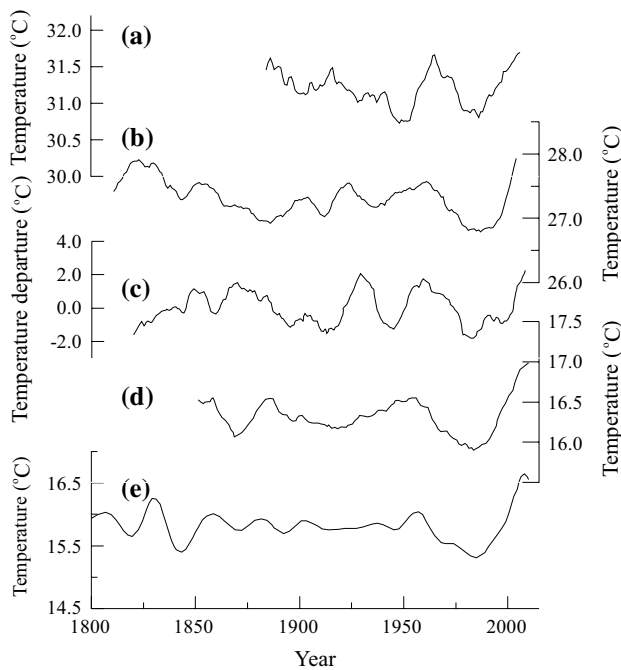
Fig. 7 Comparisons between the reconstructed temperature in SQS and other tree-ring based regional temperature reconstructions in adjacent areas. **a** June–September maximum mean temperature from Macheng, southeast China (Cai and Liu 2013); **b** this reconstruction; **c** June–September mean temperature in Daowushan, Hunan province (Shi et al. 2015a); **d** June–July mean temperature in the north of western Sichuan Plateau (Li et al. 2015a); **e** July–August mean temperature in the north western Sichuan Plateau (Xiao et al. 2015)

temperatures were subtracted. It should be stressed that the spatial representativeness of the reconstructed temperature was still exist (Fig. 6c), indicating high-frequency climatic coherence in large areas around the study area.

In order to further test the reliability of our reconstruction, as well as the spatial and temporal coherence of temperature variations in southeast China, we compared our reconstruction with other two tree-ring based growth-season temperatures in the adjacent areas: (1) the June–September maximum temperature in Macheng (MC), Hubei province (Cai and Liu 2013, Fig. 7a); (2) the June–September mean temperature in Daowushan (DWS), Hunan province (Shi et al. 2015a, Fig. 7c). All the compared series were adjusted with one-year lag to indicate the previous growth-season temperatures to keep the same timescale with our reconstruction.

The SQS temperature showed great similarity with the DWS temperature (Fig. 7b and 7c), as indicated by the spatial field analysis (Fig. 6a–c). The warm periods during 1844–1858, 1919–1926 and 1945–1965, and the cold periods during 1909–1918, 1930–1944 and 1970–2000 in SQS appeared almost synchronously in the DWS series. Moreover, the SQS temperature also showed good accordance

with the MC temperature, especially during 1920–2009 (annual scale $r = 0.282$, $p < 0.01$). We should also point out that the synchronicity of temperature variations at the early compared periods were not perfect. We speculated two possibilities: (1) the sample size at the early period of each series is comparatively low; (2) the seasons they represent are not completely the same. More reconstructions are needed to answer this difference. Excluding the early-period noise, the regional comparison leads strong support that the temperature variation in southeast China was almost synchronous at least at decadal scale.

It's worth noting that the cold period during 1970–2000 and the abrupt warming since the late 1970s were evident not only in southeast China (Fig. 7a–c), but also in the north of western Sichuan Plateau (WSP) (Li et al. 2015a; Xiao et al. 2015) (Fig. 7d, e) and the source region of the Yangtze River on the Tibetan Plateau (Liang et al. 2008). Moreover, the warm periods during 1919–1926 and 1945–1965, and the cold period during 1909–1918 in SQS were very similar to the warm period during 1934–1963 and the cold period around 1920 in the WSP (Li et al. 2015a, Fig. 7d), respectively. It may indicate a large-scale temperature synchronicity at least during recent few decades in southern China.

4.4 Linkage with the North Pacific SST and PDO

Oceans play great role on modulating air circulation and world climate change. Therefore, more and more attentions were given to the relationship between sea surface temperature (SST) and regional climate (Li 2009; Cai et al. 2015). China is adjacent to the North Pacific ocean (NP), NP-SST and related Pacific Decadal Oscillation (PDO) significantly influence climate on this vast land (Wei et al. 2004; Ma 2007), especially the adjacent southeast China. Figure 6e clearly shows that temperature variation in SQS is closely related to the SST in the central part of NP. A high SST in central NP will lead to a high temperature in SQS, and vice versa. Similar result was also reported in the tree-ring researches in the eastern Qinling Mountains (Tian et al. 2011) and other site of southeast China (Chen et al. 2015).

PDO is often described as a long-lived El Niño-like pattern of Pacific climate variability (Zhang et al. 1997). When the PDO is in a warm phase, SST in central NP will be extremely cold, and the contrary when PDO is in a cold phase (Mantua and Hare 2002; Ma 2007). Therefore, high temperature in SQS should be related to the cold-phase PDO (abnormal high SST in central NP), and low temperature to the warm-phase PDO (abnormal low SST in central NP). The PDO index (http://research.jisao.washington.edu/pdo/PDO.latest) and the reconstructed March–October maximum temperature in SQS delineated negative correlations on both annual ($r = -0.29$, $p < 0.01$) and decadal
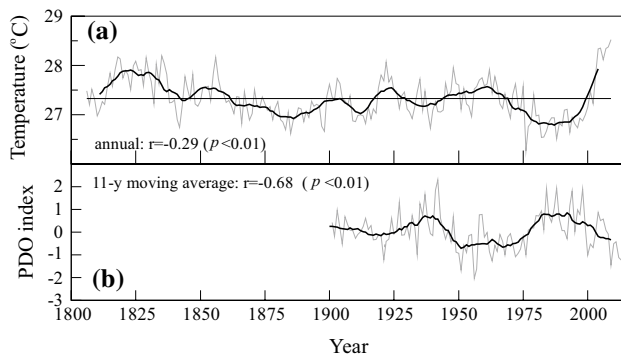
Fig. 8 Comparison between **a** the temperature reconstruction and **b** the previous March–October PDO. *Bold lines* are 11-year moving average curves

scale ($r = -0.68$, $p < 0.01$) at significant level (Fig. 8), convincingly supported the above hypothesis. Similar conclusion was also drawn in the DWS region (Shi et al. 2015a). However, the physical mechanism that how does SST in NP or PDO influence temperature variation in southeast China is unclear (Ma 2007). More researches in this area are needed in the future.

5 Conclusions

A new temperature-sensitive tree-ring width chronology from *Pinus taiwanensis* Hayata is developed in southeast China. The maximum mean temperature from previous March to previous October is correspondingly reconstructed since 1806 based on the climate-growth analysis. There are four evident cold periods (1860–1898, 1909–1918, 1930–1944 and 1970–2000) and five warm periods (1814–1837, 1844–1858, 1919–1926, 1945–1965 and 2003–2009) in the reconstruction, and 2003–2009 is the warmest period. Opposite to the warming trend of the Northern Hemisphere during the last two centuries, the temperature in SQS experienced slowly cooling from 1806 to 1980, followed by a rapid warming afterward. The reconstructed temperature in SQS not only contains local climate signal, but also shows large-scale temperature representativeness of southeast China. This work preliminary indicates that the SST variation over the North Pacific Ocean and related PDO have great impact on the temperature change in SQS. But the physical mechanism that how does SST in NP or PDO influence temperature variation in southeast China need to be studied in the future.

References

Bradley RS, Jones PD (1993) Little Ice Age summer temperature variations: their nature and relevance to recent global warming trends. Holocene 3:367–376

Büntgen U, Tegel W, Nicolussi K, McCormick M, Frank D, Trouet V, Kaplan JO, Herzig F, Heussner K-U, Wanner H, Luterbacher J, Esper J (2011) 2500 years of European climate variability and human susceptibility. Science 331:578–582

Cai QF, Liu Y (2013) The June–September maximum mean temperature reconstruction from Masson pine (*Pinus massoniana* Lamb.) tree rings in Macheng, southeast China since 1879 AD. Chin Sci Bull 58(Suppl I):169–177 **(in Chinese with English abstract)**

Cai QF, Liu Y, Liu H, Ren JL (2015) Reconstruction of drought variability in North China and its association with sea surface temperature in the joining area of Asia and Indian-Pacific Ocean. Palaeogeogr Palaeocl 417:554–560

Chen F, Yuan YJ, Wei WS, Yu SL, Zhang TW (2012) Tree ring-based winter temperature reconstruction for Changting, Fujian, subtropical region of Southeast China, since 1850: linkages to the Pacific Ocean. Theor Appl Climatol 109:141–151

Chen ZJ, Zhang XL, He XY, Davi NK, Cui MX, Peng JJ (2013) Extension of summer (June–August) temperature records for northern Inner Mongolia (1715–2008), China using tree rings. Quat Int 283:21–29

Chen F, Yuan YJ, Wei WS, Yu SL, Wang HQ (2015) Tree-ring response of subtropical tree species in southeast China on regional climate and sea-surface temperature variations. Trees 29:17–24

Christiansen B, Ljungqvist FC (2012) The extra-tropical Northern Hemisphere temperature in the last two millennia: reconstructions of low-frequency variability. Clim Past 8:765–786

Cook ER (1985) A time-series analysis approach to tree-ring standardization. Dissertation for the Doctoral Degree. The University of Arizona, Tucson

Cook ER, Kairiukstis LA (1990) Methods of dendrochronology: applications in the environmental sciences. Kluwer, Dordrecht

Cook ER, Meko DM, Stahle DW, Cleaveland MK (1999) Drought reconstructions for the continental United States. J Clim 12:1145–1162

Cook ER, Krusic PJ, Anchukaitis KJ, Buckley BM, Nakatsuka T, Sano M (2013) Tree-ring reconstructed summer temperature anomalies for temperate East Asia since 800 CE. Clim Dyn 41(11–12):2957–2972

Davi NK, D'Arrigo RD, Jacoby GC, Cook ER, Anchukaitis KJ, Nachin B, Rao MP, Leland C (2015) A long-term context (931–2005 C.E.) for rapid warming over Central Asia. Quat Sci Rev 121:89–97

Ding YH, Wang ZY, Song YF, Zhang J (2008) The unprecedented freezing disaster in January 2008 in southern China and its possible association with the global warming. Acta Meteorol Sin 22:535–558

Duan JP, Zhang QB, Lv LX, Zhang C (2012) Regional-scale winter-spring temperature variability and chilling damage dynamics over the past two centuries in southeastern China. Clim Dyn 39:919–928

Duan JP, Li L, Fang YJ (2015) Seasonal spatial heterogeneity of warming rates on the Tibetan Plateau over the past 30 years. Sci Rep 5:11725. doi:10.1038/srep11725

Esper J, Cook ER, Schweingruber FH (2002) Low frequency signals in long tree-ring chronologies for reconstructing past temperature variability. Science 295:2250–2253

Fang KY, Gou XH, Chen FH, Li JB, D'Arrigo R, Cook E, Yang T, Davi N (2010) Reconstructed droughts for the southeastern Tibetan Plateau over the past 568 years and its linkages to the Pacific and Atlantic Ocean climate variability. Clim Dyn 35(4):577–585

Fritts HC (1976) Tree rings and climate. Academic Press, London

Ge QS (2011) The climate change in China during the past dynasties. Science Press, Beijing, pp 1–709

Gong GF, Zhang PY (1983) The historical frozen injuries of citrus. Agricultural press, Beijing

He Y, Fan GF, Zhang XW, Gao DW, Hu B (2012) Vegetation phenology monitoring and spatio-temporal dynamics in Zhejiang province in past 10 years. Chin Agric Sci Bull 28(16):117–124

Holmes RL (1983) Computer-assisted quality control in tree-ring dating and measurement. Tree Ring Bull 43:69–75

Li JP (2009) Tropical pacific and its global impacts. Theor Appl Climatol 97:1–2

Li LL, Shi JF, Hou XY, Ye JS, Mao HB, Zhao XW, Lu HY (2014) High altitude *Pinus taiwanensis* Hayata growth response to climate in Jiulongshan and Guniujiang, Southeastern China. Chin J Appl Ecol 7:1849–1856

Li JJ, Shao XM, Li YY, Qin NS, Yang T (2015a) The relationship between early summer air temperature and the global sea surface temperature in the north of western Sichuan Plateau from 1854 to 2010. J Desert Res 35(4):1024–1035 **(in Chinese with English abstract)**

Li Q, Liu Y, Song HM, Yang YK, Zhao BY (2015b) Divergence of tree-ring-based drought reconstruction between the individual sampling site and the Monsoon Asia Drought Atlas: an example from Guancen Mountain. Sci Bull 60(19):1688–1697

Liang EY, Shao XM, Qin NS (2008) Tree-ring based summer temperature reconstruction for the source region of the Yangtze River on the Tibetan Plateau. Glob Planet Change 61:313–320

Liang EY, Liu B, Zhu LP, Yin ZY (2011) A short note on linkage of climatic records between a river valley and the upper timberline in the Sygera Mountains, southeastern Tibetan Plateau. Glob Planet Change 77:97–102

Linderholm HW, Björklund J, Seftigen K, Gunnarson BE, Fuentes M (2015) Fennoscandia revisited: a spatially improved tree-ring reconstruction of summer temperatures for the last 900 years. Clim Dyn 45:933–947

Liu Y, An ZS, Linderholm HW, Chen DL, Song HM, Cai QF, Sun JY, Tian H (2009) Annual temperatures during the last 2485 years in the mid-eastern Tibetan Plateau inferred from tree rings. Sci China Ser D Earth Sci 52(3):348–359

Liu Q, Wu X, Ma J, Li T, Zhou X, Guo T (2013) Effects of high air temperature on rice grain quality and yield under field condition. Agron J 105(2):446–454

Ma ZG (2007) The interdecadal trend and shift of dry/wet over the central part of North China and their relationship to the Pacific Decadal Oscillation (PDO). Chin Sci Bull 52(15):2130–2139

Mann ME, Zhang ZH, Rutherford S, Bradley RS, Hughes MK, Shindell D, Ammann C, Faluvegi G, Ni FB (2009) Global signatures and dynamical origins of the Little Ice Age and Medieval climate anomaly. Science 326:1256–1260

Mantua NJ, Hare ST (2002) The Pacific decadal oscillation. J Oceanogr 58:35–44

Matthews JA, Briffa KR (2005) The 'Little Ice Age': reevaluation of an evolving concept. Geogr Ann 87(1):17–36

McCarroll D, Loader NJ (2004) Stable isotopes in tree rings. Quat Sci Rev 23:771–801

Meko DM, Graybill DA (1995) Tree-ring reconstruction of Upper Gila River discharge. Water Resour Bull 31:605–616

Michael EM (2003) Little Ice Age. In: MacCracken MC, Perry JS (eds) Encyclopedia of global environmental change, Volume 1, The Earth system: physical and chemical dimensions of global environmental change, pp 504–509

Osborn TJ, Briffa KR, Jones PD (1997) Adjusting variance for sample-size in tree-ring chronologies and other regional mean time-series. Dendrochronologia 15:89–99

PAGES 2 K Consortium (2013) Continental-scale temperature variability during the past two millennia. Nat Geosci 6:339–346

Pan RZ (2007) Plant physiology, 5th edn. Higher Education Press, Beijing, pp 1–321

Rotenberg E, Yakir D (2010) Contribution of semi-arid forests to the climate system. Science 327(5964):451–454

Seftigen K, Linderholm HW, Drobyshev I, Niklasson M (2013) Reconstructed drought variability in southeastern Sweden since the 1650s. Int J Climatol 33:2449–2458

Shi JF, Cook ER, Lu HY, Li JB, Wright WE, Sheng FL (2010) Tree ring based winter temperature reconstruction for the lower reaches of the Yangtze River in southeast China. Clim Res 41:169–175

Shi F, Yang B, Mairesse A, Gunten LV, Li JP, Bräuning A, Yang FM, Xiao X (2013) Northern Hemisphere temperature reconstruction during the last millennium using multiple annual proxies. Clim Res 56(3):231–244

Shi JF, Li LL, Han ZY, Hou XY, Shi SY (2015a) Tree-ring width based June–September temperature reconstruction and its teleconnection with PDO and ENSO in Mount Daowu, Hunan province. Quat Sci 35(5):1155–1164 **(in Chinese with English abstract)**

Shi PH, Tang L, Wang LH, Sun T, Liu LL, Cao WX, Zhu Y (2015b) Post-heading heat stress in rice of South China during 1981–2010. PLoS ONE 10(6):e0130642. doi:10.1371/journal.pone.0130642

Suehrcke H (2000) On the relationship between duration of sunshine and solar radiation on the earth's surface: Ångström's equation revisited. Sol Energy 68(5):417–425

Tian QH, Zhou XJ, Liu Y, Zhao P (2011) Historical late-spring-to-early-summer temperature at Qinling Mountain range inferred from multi-site tree-ring chronologies, and their relationship with Northern Hemisphere sea surface temperature. Quat Sci 31(5):864–872 **(in Chinese with English abstract)**

Wang SW, Ye JL, Gong DY (1998) Climate in China during the Little Ice Age. Quat Sci 1:54–63 **(in Chinese with English abstract)**

Wei J, Yang H, Sun SQ (2004) Relationship between the anomaly longitudinal position of subtropical high in the western Pacific and sever hot weather in North China in summer. Acta Meteorol Sin 62(3):308–316 **(in Chinese with English abstract)**

Wigley TML, Briffa KR, Jones PD (1984) On the average value of correlated time series, with applications in dendroclimatology and hydrometeorology. J Appl Meteorol Clim 23:201–213

Xiao DM, Qin NS, Huang XM (2015) A 325-year reconstruction of July–August mean temperature in the North of west Sichuan derived from tree-ring. Quat Sci 35(5):1134–1144 **(in Chinese with English abstract)**

Xing P, Zhang QB, Lv LX (2014) Absence of late-summer warming trend over the past two and half centuries on the eastern Tibetan Plateau. Glob Planet Change 123:27–35

Yadav RR, Singh J (2002) Tree-ring-based spring temperature patterns over the past four centuries in western Himalaya. Quat Res 57:299–305

Yadav RM, Park WK, Bhattacharyya A (1999) Spring-temperature variations in western Himalaya, India, as reconstructed from tree-rings: AD 1390–1987. Holocene 9(1):85–90

Yadav RR, Park WK, Singh J, Dubey B (2004) Do the western Himalayas defy global warming? Geophys Res Lett 31:L17201. doi:10.1029/2004GL020201

Yang B, Qin C, Wang JL, He MH, Melvin TM, Osborn TJ, Briffa KR (2014) A 3,500-year tree-ring record of annual precipitation on the northeastern Tibetan Plateau. PNAS 111(8):2903–2908

Ye Q, Yang XG, Dai SW, Chen GS, Li Y, Zhang CX (2015) Effects of climate change on suitable rice cropping areas, cropping systems and crop water requirements in southern China. Agr Water Manage 159:35–44

Yin GS, Yang MG, Ma ZX, Liu XY, Yang YG, Long MM (2007) Study on "Mount Sanqingshan-type" granite geology and landscapes. Geol Rev S1:56–74 **(in Chinese with English abstract)**

Zhang QB, Evans MN, Lyu LX (2015) Moisture dipole over the Tibetan Plateau during the past five and a half centuries. Nat Commun 6:8062. doi:10.1038/ncomms9062

Zhang Y, Wallace JM, Battisti DS (1997) ENSO-like interdecadal variability: 1900–93. J Clim 10:1004–1020

Zheng JY, Ge QS, Fang XQ (2002) Seeing the 20th century warming from temperature changes of winter-half-year in eastern China for the last 2000 years. Acta Geogr Sin 57(6):631–638

Zheng YH, Zhang Y, Shao XM, Yin ZY, Zhang J (2012) Temperature variability inferred from tree-ring widths in the Dabie Mountains of subtropical central China. Trees 26:1887–1894